Original article

Research on the optimization formula performance and dust reduction effect of mine dust suppressant based on response surface method

Na Gao[1,2]*, Tianqin Zhou[1,2], Longzhe Jin[1,2], Jingguang Fan[3,4], Linquan Tong[3,4]*, Bowen Zhang[1,2]

[1]*School of Civil and Resource Engineering, University of Science and Technology Beijing, Beijing 100083, P. R. China*

[2]*State Key Laboratory of High-Efficient Mining and Safety of Metal Mines (University of Science and Technology Beijing), Ministry of Education, Beijing 100083, P. R. China*

[3]*National Center for Occupational Safety and Health, NHC, Beijing 102308, P. R. China*

[4]*NHC Key Laboratory for Engineering Control of Dust Hazard, Beijing 102308, P. R. China*

Abstract:
In this study, sodium dodecyl benzene sulfonate, triton, guar gum and sodium polyacrylate are selected as the composite raw materials of dust suppressants through the determination of physical and chemical properties of single components. Design expert software is used to carry out the mixture design, the determination of experimental parameters and the response surface analysis of the sedimentation rate, evaporation resistance property, surface tension, contact angle of coal dust with the reagent. According to the response surface analysis results, the optimal ratio of the reagent has been determined, which is 39.8% for sodium dodecyl benzene sulfonate, 53% for triton, 3.9% for guar gum, and 3.3% for sodium polyacrylate. The results of infrared spectrum show that the dust suppressant had a significant effect on the content change of hydroxyl of hydrophilic functional groups of coal dust. The results of scanning electron microscope experiments show that the dust suppressor has good wetting and binding effects on coal dust. The toxicity test shows that the coal sample did not have the acute inhalation toxicity characteristics of hazardous waste. The dust reduction experiment in similar space shows that the dust reduction efficiency of this new dust suppressants is 95.3%, which is 28.1% and 10.2% higher than that of natural dust fall and water spray dust fall. The conclusions of this study are of great significance for improving the dust reduction efficiency of mine dust suppressants, the dust prevention technologies, the working environment of underground workers, and reducing the incidence of pneumoconiosis.

1. Introduction

In the process of coal mining, dust explosion accidents (Azam and Mishra, 2019; Rolf and Li, 2021; Ray et al., 2022) occur from time to time, which lead to many derivative accidents (Kumykov and Kumykova, 2013; Eades et al., 2018; Perera et al., 2021) and serious consequences. The concentration of coal mining dust exceeding the relevant national standards is the main reason for the explosion and secondary explosion in the mine. China is a major coal producer (Zhang et al., 2021), the domestic pneumoconiosis (Li et al., 2019; Wang et al., 2021) patients account for 90% of the occupational disease patients. More than 90% of the pneumoconiosis patients are concentrated in the coal industry. According to the judgment standard for the management limit of dust exposure concentration in the coal mine workplace in China, when the content of free silica in the dust is less than 10%, the maximum allowable concentration of total dust is 10 mg/m^3, and the maximum allowable concentration of respiratory dust is 3.5 mg/m^3. In the coal mine excavation face, the dust

*Corresponding author.
E-mail address: aggie198308@163.com (N. Gao); ztq990710@163.com (T. Zhou); lzjin@ustb.edu.cn (L. Jin); fan-jg@263.net (J. Fan); tlqzyzx@163.com (L. Tong); 18810316889@163.com (B. Zhang).

concentration is far higher (Pan et al., 2021) than the specified concentration, which not only harms the health of coal miners, but also has serious safety hazards. Therefore, it is necessary to carry out the research on dust technologies and methods (He et al., 2023). Dust suppressants are considered one of the most effective methods for mine dust removal.

Anionic surfactant sodium dodecylbenzene sulfonate (Geetha et al., 2010) can serve as a wetting agent component in chemical dust suppressants. It is also often mixed with other surfactants or inorganic salts (Abdel Rahem, 2023; Dudek et al., 2023) as a wetting agent for mine dust reduction. The mixture of wetting agent can play a synergistic role and improve the hydrophilicity of coal powder. Shi et al. (2019) found that sodium dodecylbenzene sulfonate interacts synergistically with primary alcohol ethoxylate and ethylene glycol polyoxyethylene ether after being combined. After dust suppression treatment of raw coal, the hydrophilicity of coal powder can be improved. The nonionic surfactant triton (Amato et al., 2010; Tessum and Raynor, 2017) can improve the efficiency of coal dust collection to a certain extent and exhibit good performance in coal dust collection. Zhou et al. (2018) proposed a dust suppressant composed of a mixture of 0.7% water-soluble polymer and 0.1% Triton X-100, which can adhere to fine brown coal particles through solid bridging force to form a polymer protective film. Sodium polyacrylate (Sah and Dutta, 2010; Sartore et al., 2017) has good water absorption and retention properties. Huang et al. (2021) prepared a new type of dust suppressant by using sodium polyacrylate, sodium carbonate, polyethylene glycol, and alkyl glycosides as raw materials. After 10 days later, the water content can be maintained at 4% to 5% at room temperature. Shao et al. (2023) and others found that -COO- and -OH in sodium alginate form a synergistic effect with the hydrophilicity of -CO- and -COOH in sodium polyacrylate, which can enhance the water absorption of sodium polyacrylate. Guar gum can improve the flocculation characteristics of copolymers. Zhang et al. (2020) synthesized hydroxypropyl guar gum by using guar gum and epoxy propane, which increase the average dust removal rates of total dust and inhalable dust to 83.94% and 84.08%, respectively. Smita et al. (2022) utilized the nontoxic and environmentally friendly properties of guar gum to synthesize trimethylammonium chloride grafted guar gum, which was optimized as a flocculant for ore treatment and showed excellent flocculation effects for kaolin and iron ore.

The orthogonal design method is commonly adopted when conducting the research on multi-component formula of dust suppressant. Rakhi et al. (2021) utilized orthogonal design method to investigate the hydroxypropylation reaction of guar gum, synthesized derivatives under optimized conditions. The hydroxypropyl derivative obtained exhibited better thermal stability than natural guar gum. Yang et al. (2021) optimized the components of a dust suppressant through orthogonal experiment, obtained an environmental, biodegradable straw dust suppressant with excellent dust suppression performance. However, linear model adopted by orthogonal design is difficult to fit binomial function relationship. Therefore, some researchers have begun to use response surface design method to fit binomial and polynomial function relationships for the

mutual influence of multicomponent reagent formulas in order to confirm the optimize formula components. Alrweilih et al. (2020) optimized the response surface design method. Chaker et al. (2021) optimized an efficient statistical modeling of response surface method and proposed a new photodegradation material of textile azo dyes. Liang et al. (2022) used response surface method to optimize the proportion of four cellulases and the proportion of dust inhibitor additives. Through the simulation spray test, the dust suppression efficiency of PM10 and PM2.5 was increased to 93.7% and 91.5% respectively. Li et al. (2023) proposed a optimization model of response surface method based for the ratio of dust suppressants. The optimization model was used to fit multiple linear relationship of the dust suppressant components. The settling time of dust suppressants is actually reduced by 23% compared to water dust suppression.

There are various types of chemical dust suppressants (Tsai et al., 2020; Kunz et al., 2021), which have significant dust suppression effects (Luo et al., 2016; Xi et al., 2017; Tsogt and OH, 2021). However, there are still some problems with existing mine dust suppression. Dust quickly dries out after gravity settling, which causes secondary dust. The high cost of each component in the dust suppressant formula causes a challenge in promoting its application on-site. Existing studies predominantly focus on enhancing dust suppression efficiency, often neglecting the safety of dust suppressants for underground workers. The research on efficient and nontoxic mine dust suppressant is necessary. Kan et al. (2017) proposed that over 80% of coal dust particles in excavation and fully mechanized mining faces range in size from 0.100 to 0.150 mm (Wang et al., 2024). According to GB/T6003.1-2017, dust particles ranging in size from 0.106 to 0.150 mm are defined as 100 mesh. Therefore, in this study, 100 mesh coal dust was selected as the research object (Qiu et al., 2023). Composite raw materials are based on the commonly used dust suppressant raw materials according to the relevant references mentioned in the last paragraph. By conducting performance experiments, settling efficiency, water retention, conductivity performance, surface tension, and contact angle of dust suppressant formula are tested. The optimal ratio of the effective and nontoxic dust suppressant formula is determined by using Design Expert software, and response surface analysis method. The optimized reagent is characterized through infrared spectroscopy and scanning electron microscopy to explain the mechanism of new dust suppressant improving the wetting performance of coal dust. A similar experimental system is established to simulate the underground environment and verify the new dust suppressant reduction efficiency.

2. Materials and methods

2.1 Materials

2.1.1 Coal sample preparation

All coal samples were obtained from a mechanized mining face of a coal mine in Anhui Province. The required coal blocks were taken at the front of the comprehensive excavation tunnel. The coal block was grinded to the required particle size

Table 1. Materials used in the experiment.

Type	Reagent name	Molecular formula
Wetting agent	Sodium dodecyl sulfate	$C_{12}H_{25}SO_4Na$
	Dodecyl trimethyl ammonium chloride	$C_{12}H_{25}(CH_3)_3NCl$
	Triton	$C_{34}H_{62}O_{11}$
Adhesive agent	Sodium dodecyl benzene sulfonate	$C_{18}H_{29}NaO_3S$
	Guar gum	$C_{10}H_{14}N_5Na_2O_{12}P_3$
	Sodium carboxy methyl cellulose	$[C_6H_7O_2(OH)_2OCH_2COONa]_n$
Water-retaining agent	Sodium polyacrylate	$(C_3H_3NaO_2)n$
	Absorbent resin particles	$C_6H_{10}NaO_9P$
	Hydroxypropyl cellulose	$[C_6H_7O_2(OCH_2CHOH)x(OH)_{3-x}]nCH_3$

Weigh → Pour → Settlement → Timing
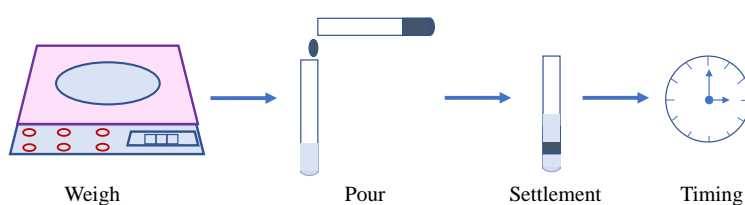
Fig. 1. Wetting agent experiment process.

by using a ball mill. The coal dust utilized in this experiment was sieved through a 100-mesh sieve.

2.1.2 Reagent preparation

The statistics for the drugs used in this study, including the type, the name and the molecular formula of each drug, are shown in Table 1.

2.2 Single component experiment

2.2.1 One-component wetting agent experiment

(1) Experiment preparation

Using an electronic balance, 72 portions of 0.5 grams of 100 mesh coal powder were weighed. The weighted coal powder were poured into individual test tubes to ensure consistent horizontal height. According to the research conclusions of Zhao et al. (2023), wetting agent solutions, namely SDS, DTAC, TX-100, and SDBS, were prepared with mass fractions of 0.1%, 0.5%, 1%, 2%, 5%, and 10% in this research. Each prepared solution was then poured into a corresponding test tube.

(2) Experiment design

As shown in the Fig. 1, the coal powder was poured into the test tubes containing different mass fractions of surfactant solution in a sequential manner. The time cost for each coal sample to settle to the same height from the liquid level in each test tube is recorded. Three parallel experiments for each test tube were conducted. Finally, the average settle time was adopted for each mass fractions agent solution.

2.2.2 Multi-component wetting agent experiment

(1) Experiment preparation

By using an electronic balance, 12 portions of 0.5 grams of 100 mesh coal powder were weighed. The weighted coal powder were poured into individual test tubes to ensure consistent horizontal height. Three mixed solutions were prepared, with 2% mass fractions of TX-100, 2% mass fractions of DTAC, 2% mass fractions of TX-100, 0.5% mass fractions of SDBS, 1% mass fractions of DTAC, 1% mass fractions of SDBS, 2% mass fractions of DTAC and 0.5% mass fractions of SDBS. The prepared solutions were poured into the corresponding test tubes as the surfactant solution.

(2) Experiment design

The prepared solutions were poured into the corresponding test tubes as the surfactant solution. The coal powder was poured into the test tubes containing different mass fractions of surfactant solution in a sequential manner. The time taken for the coal powder to settle to the same height from the liquid surface in different test tubes separately was recorded. Three parallel experiments were conducted on each different mass fractions of surfactant solution and the average value recorded in the three experiments was selected as the settling time of the coal powder in different types of surfactant solution.

2.2.3 Adhesive agent experiment

(1) Experiment preparation

A total of 5 E412 solution samples were prepared, each with a mass fraction of 0.1%, 0.2%, 0.3%, 0.4% and 0.5%, respectively. The viscosity of CMC Na is low, so prepare a solution with a higher concentration. A total of 6 CMC-Na
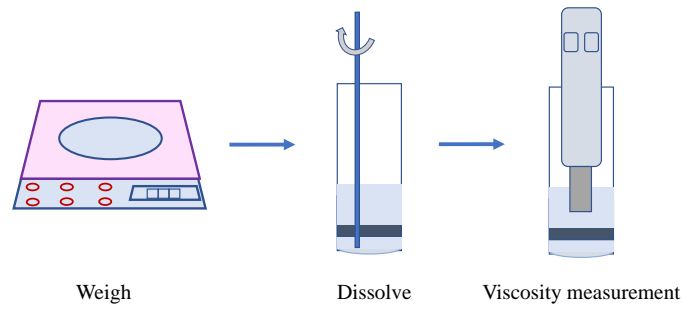
Fig. 2. Adhesive agent experiment process.
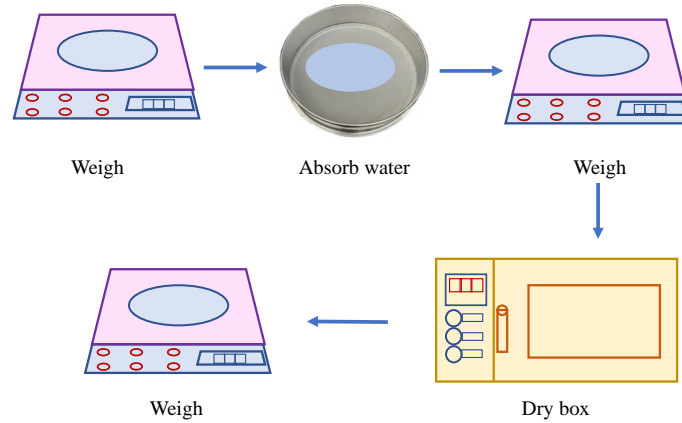
Fig. 3. Water-retaining agent experiment process.

solution samples were prepared, each with a mass fraction of 1%, 1.2%, 1.3%, 1.5%, 1.8% and 2%, respectively.

(2) Experiment design

As shown in the Fig. 2, using an electric mixer to completely dissolve the reagent at a constant temperature. The viscosity values of the solution at 25°C are measured by using the NDJ-85 rotary viscometer model with rotor 1 at a speed of 60 r/min. Each experiment was measured for three times to obtain an average value of the viscosity value for each mass fraction solution.

2.2.4 Water-retaining agent experiment

(1) Experiment preparation

In order to select one of the three types of water retaining agents PAAS, SPA, and HPC as the water retaining component of the composite dust suppressant, this study conducted a single component dust suppressant water retention experiment. Three water retaining agent samples of PAAS, SPA, and HPC have been prepared. The three samples of PAAS, SPA, and HPC were weighed by using an electronic balance with a mass of m_1. The weighed reagents were soaked in 500 ml of water until it was fully saturated.

(2) Experiment design

As shown in the Fig. 3, solid-liquid separation of the water-retaining agent was performed by passing it through a 100-mesh sieve, and the gel was weighed and recorded as m_2, the water absorption ratio Q is calculated as follow:

$$Q = \frac{m_2 - m_1}{m_1} \tag{1}$$

where Q is the water absorption ratio; m_1 is the mass of water-retaining agent before water absorption, g; m_2 is the mass of water-retaining agent after water absorption, g.

The water-retaining agent, fully saturated and in its absorbed state, was transferred to an evaporating dish after solid-liquid separation. The mass of the gel was measured and recorded as m_2. In order to determine the water retention performance of the three types of water-retaining agent in real underground coal mine environments, the gel was placed in DH-101 electric constant temperature blast drying oven at 40 °C. The mass of the gel was then measured every half an hour and recorded as m_3, the water retention rate R is calculated as follow:

$$R = \frac{m_3 - m_1}{m_2 - m_1} \tag{2}$$

where R is the water retention ratio; m_3 is the mass of water-retaining agent after losing water for a certain time, g.

2.3 Response surface analysis experiment

In this experiment, the dust reduction performances and mutual influence relationship of four agents sodium dodecyl benzene sulfonate A, triton B, guar gum C, sodium polyacrylate D were studied. The optimal ratio of each component in the composite dust suppressant was further studied through response surface analysis experiment.

Table 2. Design data of dust suppressant mixture.

No.	x_1 (%)	x_2 (%)	x_3 (%)	x_4 (%)
1	1.000	0.000	0.000	0.000
2	0.500	0.000	0.000	0.500
3	0.000	0.000	1.000	0.000
4	0.000	1.000	0.000	0.000
5	0.125	0.625	0.125	0.125
6	0.000	0.500	0.500	0.000
7	0.125	0.125	0.625	0.125
8	0.000	0.000	0.000	1.000
9	0.500	0.500	0.000	0.000
10	0.125	0.125	0.125	0.625
11	0.625	0.125	0.125	0.125
12	0.000	0.500	0.000	0.500
13	0.500	0.000	0.500	0.000
14	0.250	0.250	0.250	0.250
15	0.000	0.000	0.500	0.500

Multi-component mixing experiments models were designed by design expert software. The simplex lattice method was used to achieve different combinations of the proportions of various agents in the experiment. The independent variables x_1, x_2, x_3, and x_4 represent the concentrations (mass fractions) of sodium dodecyl benzene sulfonate (A), triton (B), guar gum (C), and sodium polyacrylate (D), respectively, while the dependent variables Y_1, Y_2, Y_3, and Y_4 represent the values of sedimentation rate, evaporation resistance, surface tension, and contact angle, respectively. The parameter levels of the independent variables (x_1, x_2, x_3, x_4) in the initial mixture design model are all 0-1, that is, the lower limit of the concentration is 0 and the upper limit is 100%.

The specific conditions for confirming the mixture model in Table 2 are as follow:

$$\sum_{i=1}^{4} x_i = x_1 + x_2 + x_3 + x_4 = 1 \qquad (3)$$

Design-expert 13 software provides 15 mixed design schemes, as shown in Table 2.

The 15 formulas designed in Table 2 are configured and diluted with water to a concentration of 0.1% to determine the values of Y_1, Y_2, Y_3, Y_4.

1) Determination of reagent sedimentation rate Y_1. The dust suppressant solution was prepared according to the designed ratio, and the surface tension of the reagent was measured. After the dust suppressant solution being configured, 0.5 g of 100 mesh coal powder was poured into the nozzle and the settling time of the coal powder was recorded. Each formula was required to be measured for three times to obtain the average value, resulting in a total of 45 samples being prepared.
2) Determination of reagent evaporation resistance Y_2. The

dust suppressant solution was prepared according to the designed ratio, and then sprayed on the dust powder samples. The dust powder samples sprayed were conducted the reagent evaporation resistance experiments. The quantitative reagent was weighed and soaked in 500 ml of water. After the reagent being fully absorbed and saturated, the solid-liquid mixture was slowly poured onto the filter screen, and the mass of the gel was filtered and weighed as m_4. The fully absorbed reagent was then placed into an evaporating dish and placed in a constant temperature oven at 40°C. It was taken out, weighed, and recorded as m_5 every half an hour. The calculation formula of water retention rate r is calculated as follow:

$$r = \frac{m_4 - m_5}{m_4} \qquad (4)$$

where r is water retention ratio; m_4 is the mass of reagent after water being absorbed, g; m_5 is the mass of reagent after losing water for a certain time, g.

3) Determination of reagent surface tension Y_3. The dust suppression agent solution was prepared according to the design ratio, and the reagent surface tension was measured by using the JYW-200B automatic interface tension meter. The surface tension meter was placed on a horizontal surface, and the probe was heated with an alcohol lamp. The probe was hung on the microbalance of the surface tension meter, and the data was calibrated with pure water. This step was repeated to measure the surface tension of different formula solutions. The average of each group of reagents is calculated by conducting 4 measurements experiments.
4) Reagent dynamic contact angle Y_4. The dust suppression agent solution was prepared according to the design ratio, and the dynamic contact angle was measured by using the ThetaLite101 contact angle tester and the 769YP-24B powder tablet press. 0.7 g of coal powder was taken and poured into the tablet mold. The pressure was adjusted to 10 MPa, and the coal powder was pressed into a tablet. These steps were repeated to prepare 45 coal tablet samples. The contact angle tester was used to measure the dynamic contact angle between the dust suppressant solutions of different ratios and the surface of coal sheets.

2.4 Characterization experiment

Taking into account the impact of dust suppressant concentration on the on-site reagent addition equipment of the fully mechanized mining face, in this study, the reagent was diluted with water to a concentration of 0.1% after the proportion of the dust suppressant concentration being selected.

1) Infrared spectrum (IR) characterization. In order to study the effect of dust suppressant concentration on coal dust functional groups within the range of 0.1%-1.1%, three types of dust suppressant concentrations were selected as comparative experimental objects in IR experiments, namely 0.2%, 0.5%, and 1.0%. By analyzing the infrared spectral images of 0.2% concentration dust suppressant and coal dust, the influence of low concentration dust
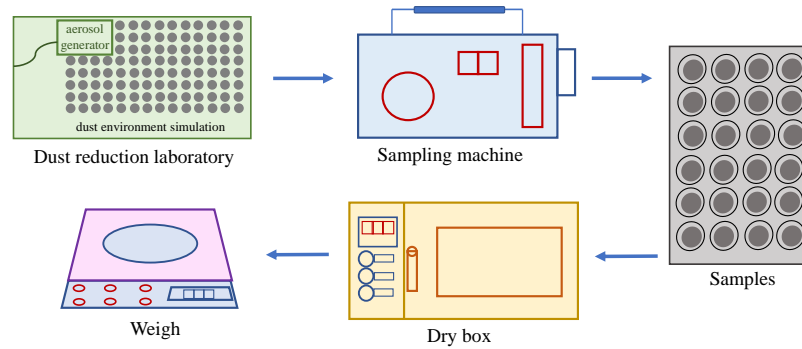
Fig. 4. Dust suppression efficiency test process.

suppressants in the range of 0.1% to 0.3% on the functional groups of coal dust can be analyzed; by analyzing the infrared spectral images of dust suppressants at a concentration of 0.5% and coal dust, the influence of higher concentrations of dust suppressants in the range of 0.4% to 0.6% on the functional groups of coal dust can be analyzed; analyze the effect of high concentration dust suppressants in the range of 0.9% to 1.1% on the functional groups of coal dust through infrared spectral images of 1.0% concentration dust suppressants and coal dust. There were two types of pulverized coal to be prepared. One is the 100-mesh coal sprayed with dust suppression agent solutions at the concentrations of 0.2%, 0.5% and 1% separately and the other one is not sprayed with any dust suppression agent. These samples, both sprayed and unsprayed, were pressed into thin slices and placed on the Nicolet IS50 Fourier transform infrared spectrometer for infrared verification. The scanning range for the spectra was set to 650-4,000 cm^{-1}. After the infrared spectrum experiment, PeakFit and Omnic software were utilized to perform peak separation and labeling analysis on the obtained spectra, aiming to investigate the changes in functional groups during the reaction process.

2) The Scanning Electron Microscope (SEM) characterization. All the coal samples were divided into two groups. One was sprayed with water and the other one was sprayed with dust suppressant. The amount of water is the same as the dust suppressant. The two groups of samples were then placed in a thermostatic drying oven and subjected to a constant temperature of 40 °C for 10 hours to ensure thorough drying. After drying, the two groups of coal samples were gold-plated and examined by using the Zeiss evo 18 Scanning Electron Microscope. According to the research results of Deng et al. (2023), in SEM studies, for objects containing 100-200 particles in a field of view, magnification of 100-200 times can meet the observation of particle gaps. During the test, the two groups of coal samples were magnified to 200 times and 300 times respectively by regulus 8,100 cold field Scanning Electron Microscope to compare and observe the changes of surface morphology of the coal samples after spraying water and dust suppressant.

3) Determination of toxicity property. The dust suppressant solution was prepared for toxicity experiment. Taking Sprague dawley rats (SD rats) as experimental animals, the limit test method was adopted. Six SD rats were put into two boxes and a static poisoning cabinet for poisoning at one time. The volume of the laboratory poisoning cabinet was 300 L. The 6.0 g sample of dust suppressant solution was added from the dosing window into the evaporation tray of the poisoning cabinet. The evaporation temperature was set at 45 °C, and the limited concentration of suppressant solution was maintained at 20 mg/L. It is then inhaled for 4 hours at a time. The weight of each SD rat have been measured and recorded starting from the day before exposure (day 0), and subsequently on the 1st, 3rd, and 7th days (and every week thereafter) to the last day of exposure. The weight of SD rat was recorded additionally on the day of death or euthanasia. A gross anatomy examination was conducted on the deceased SD rats, and the gross pathological changes of each SD rat were recorded for a period of 14 days.

2.5 Dust reduction simulation experiment

The test system which is similar to the site conditions of the fully mechanized tunnel is constructed, with dimensions of $5 \times 3 \times 2$ m^3. A steel frame and a glass transparent space are used to simulate the tunnel for the test. The specific experimental steps are illustrated in Fig. 4.

Utilizing an aerosol generator, coal dust was sprayed for a duration of 5 minutes in order to ensure the concentrations of the three stages experiment space were the same. Subsequently, a waiting period was observed to allow the pulverized coal to disperse throughout the entire experimental space. A total of five experimental measuring points were set to monitor changes of dust concentration in the experimental space. Dust samplers were employed to collect coal dust samples by covering the filter membranes on the samplers. Taking point 1 as an example, the weight of the filter membrane for the 1st time was measured and recorded as m_{110} before being covered on the dust sampler. After the filter membrane adsorbing coal dust, it was weighted and recorded as m_{111} by drying and weighting operation. The concentration of the point 1 at the 1st time C_{11} was calculated a as follow:
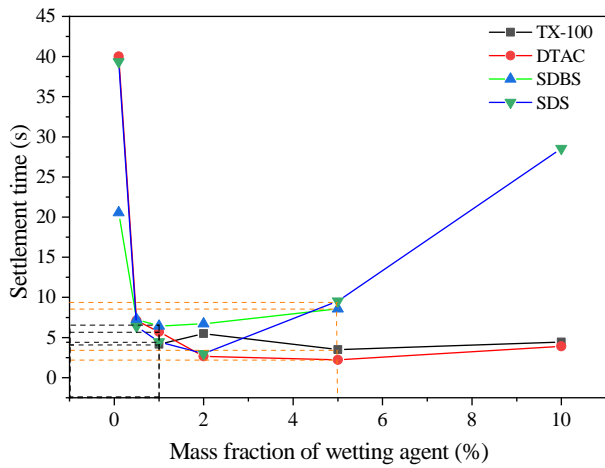
Fig. 5. Agent sedimentation rate with one-component wetting agent.

$$C_{nm} = \frac{m_{nm1} - m_{nm0}}{ft} \qquad (5)$$

where C_{nm} is coal dust concentration of point n at the m_{th} time, mg/m^3, m_{nm1} is the quality of filter membrane after sampling and drying for point n at the m_{th} time, mg, m_{nm0} is the filter membrane quality before sampling for point n at the m_{th} time, mg, f is samples flow, L/min (taking 20 L/min here), t is the time of sampling, min (taking 1 minute here).

The average value of concentration C_n for the five points were calculated as the concentration of the whole experiment space at the time. The initial concentration of the whole experiment space was recorded as C_0. The duration of the dust suppression reduction test is set to 20 minutes. Within this timeframe, the filter membranes of the five dust samplers were replaced every 5 minutes. The last time concentration of the whole experiment space was calculated as C_4. The calculation formula of dust reduction is calculated as follow:

$$\eta = \frac{C_0 - C_4}{C_4} \times 100\% \qquad (6)$$

where η is dust reduction efficiency, %, C_0 is initial dust concentration, mg/m^3, C_4 is dust concentration after 20 minutes of dust fall, mg/m^3. The dust reduction simulation experiment is designed three stages: Coal dust natural sedimentation, water spray coal dust sedimentation, dust suppressant spray coal dust sedimentation.

1) Performance testing of coal dust natural sedimentation. In this stage experiment, there was not any dust reduction measure to be conducted. The concentration of the whole experiment space was measured and calculated according to the steps above, which were recorded as CZ_0-CZ_4. And the dust reduction efficiency was calculated to be η_z.

2) Performance testing of water spray dust sedimentation. In this stage experiment, the method of spraying water is adopted to reduce dust. The concentration of the whole experiment space was measured and calculated according to the steps above, which were recorded as CS_0-CS_4. And the dust reduction efficiency was calculated to be η_S.

3) Performance testing of dust suppressant spray dust sedimentation. In this stage experiment, the method of

spraying dust suppressants is adopted to reduce dust. The concentration of the whole experiment space was measured and calculated according to the steps above, which were recorded as CY_0-CY_4. And the dust reduction efficiency was calculated to be η_Y.

3. Results and discussion

3.1 Performance analysis of the single component

3.1.1 Performance analysis of wetting agent

(1) One-component wetting agent
The change curves of the sedimentation time with the mass fraction of wetting agents (TX-100, DTAC, SDBS, SDS) are shown in Fig. 5.

As it can be seen from Fig. 5, when the reagent mass fraction is within the range of 0 to 1%, the settling time of pulverized coal decreases at a faster rate. When the reagent mass fraction exceeds 1%, the settling time of pulverized coal slowly increases with the increase of the mass fractions of SDBS and TX-100, while the settling time of pulverized coal continues to decrease when the mass fractions of SDS and DTAC are within the range of 1% to 2%. When the reagent mass fraction is 2% to 5%, the settling time of pulverized coal is proportional to the mass fractions of SDBS and SDS reagents, and inversely proportional to the mass fractions of DTAC and TX-100 reagents. Overall, when the reagent mass fraction is 1%-5%, the reagent plays a good performance of sedimentation. When the reagent mass fraction reaches 10% or more, the solution will produce a lot of foam and become viscous, and the sedimentation rate will slow down accordingly.

By comparing the settling time and clarification effect of the four reagents, it can be seen that the settling time of the four single component wetting agents with the same proportion on coal dust is ranked from fast to slow is: DTAC, TX-100, SDBS, SDS. Within the same settling time, SDBS can make coal dust agglomerate and slowly settle, and the solution can quickly recover and clarify after settling. It indicated that SDBS has a good settling effect on coal dust. Single component wetting agent is difficult to meet the requirements for efficient and rapid settling of coal dust. Therefore, further research on multi-component wetting agents is needed.

(2) Composite wetting agents
Based on the results in the paragraph of one-component agent, TX-100 and DTAC exhibit short settling time, while SDBS demonstrates effective clarification, and SDS shows poor settling performance. In order to enhance the wetting performance of the wetting agent, achieve both a short settling time and excellent clarification effects, the anionic surfactant SDBS and the non-ionic surfactant TX-100 were selected as components for the composite wetting agent. In the composite wetting agent, a portion of the anionic wetting agent SDBS binds with the hydrophobic groups on the coal powder surface. The other portion of the anionic wetting agent SDBS binds with the hydrophilic groups on the coal powder surface and then combines with the nonionic surfactant TX-100. This pro-
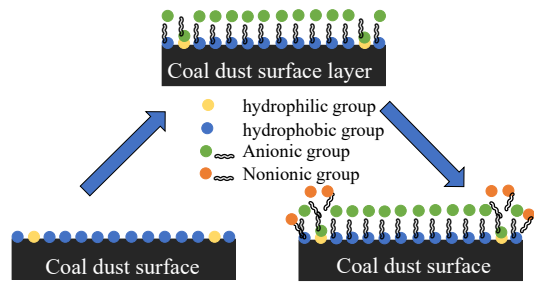
Fig. 6. Effect of different ionic surfactants on coal dust.
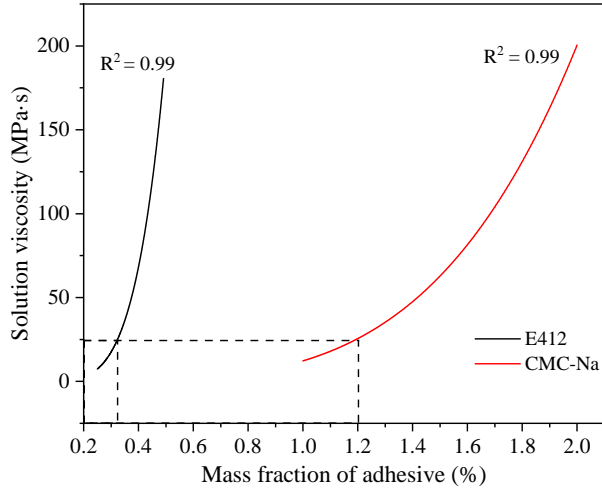
Fig. 7. Mass fraction-viscosity curves of adhesive.

cess reduces the hydrophobicity of the coal powder surface and enhances its hydrophilicity (Fig. 6). Consequently, the mixed solution of SDBS and TX-100 can increase the hydrophilicity of the coal surface, making coal dust more easily wettable (Wu et al., 2023). Based on the above principles, settling rate and clarification effects of coal powder in the mixed solution with wetting agent are improved.

3.1.2 Performance analysis of adhesive

The viscosity change curves with different mass fractions E412 and CMC-Na are shown in Fig. 7.

As it is shown in Fig. 7, both E412 and CMC-Na have good bonding effects, and the mass fraction of E412 required to achieve the same viscosity is far lower than the mass fraction of CMC-Na. From the perspective of cost control, E412 is selected as the bonding agent.

The bonding strength and cohesiveness between particles and coal dust increase with the viscosity of the dust suppressant. However, to achieve spray, the viscosity value of the dust suppressant must not be too high. Therefore, the method of response surface analysis was selected to adjust and ensure the maximum cohesiveness and appropriate solution viscosity of the dust suppressant solution with wetting agent, adhesive and water-retaining agent.

3.1.3 Performance analysis of water-retention agent

The water absorption and moisturizing effect curves of water retention agents PAAS, SPA, and HPC obtained from

Table 3. Design and experimental data of dust suppressant mixture.

No.	Y_1 (mg/s)	Y_2 (%)	Y_3 (mN/m)	Y_4 (°)
1	9.1	72.5	31	20
2	2.5	87.0	42	61
3	0.4	82.5	83	85
4	5.3	81.0	27	32
5	4.8	86.0	35	35
6	2.2	88.5	44	49
7	1.2	86.5	72	44
8	0.7	89.5	85	82
9	7.2	81.0	28	22
10	1.4	87.0	69	48
11	6.1	83.0	38	30
12	2.0	88.5	39	38
13	2.2	80.0	45	45
14	2.8	87.5	38	42
15	0.6	88.5	81	83

the experiment are shown in Fig. 8.

From Fig. 8, it can be seen that the PAAS has the most stable moisture absorption performance in the three water retaining agents PAAS, SPA, and HPC. (Fig. 8(a)). The experimental and calculated water retention curves of the reagents indicate that, after the same drying time, the water retention rate of PAAS is significantly better than that of SPA and HPC (Fig. 8(b)). Therefore, PAAS was chosen as the water retention agent.

3.2 Analysis of response surface result

The determination results of the 15 mixture models of four reagents and related experimental data are shown in Table 3.

It can be seen that the increase of the types of ingredients improved the comprehensive performance of the dust suppressant. The physical and chemical properties of the dust suppressant solution related to pulverized coal vary greatly with the change of the ingredients proportion. Different agents have different effects on the property of dust suppressant. There are four factors that can reflect the performance of dust suppressants which are sedimentation rate, evaporation resistance, surface tension and contact angle. This study used reaction surface analysis to determine the optimal ratio of composite dust suppressant agents that can ensure the best performance of the dust suppressant.

Data fitting analysis was conducted by using the concentrations of four reagents x_1, x_2, x_3, x_4 as independent variables and the values of four performances Y_1, Y_2, Y_3 and Y_4 as dependent variables. And the correlation coefficient R^2 was calculated.

The multivariate linear equation fitting the sedimentation rate of dust is ($R^2 = 0.98$):
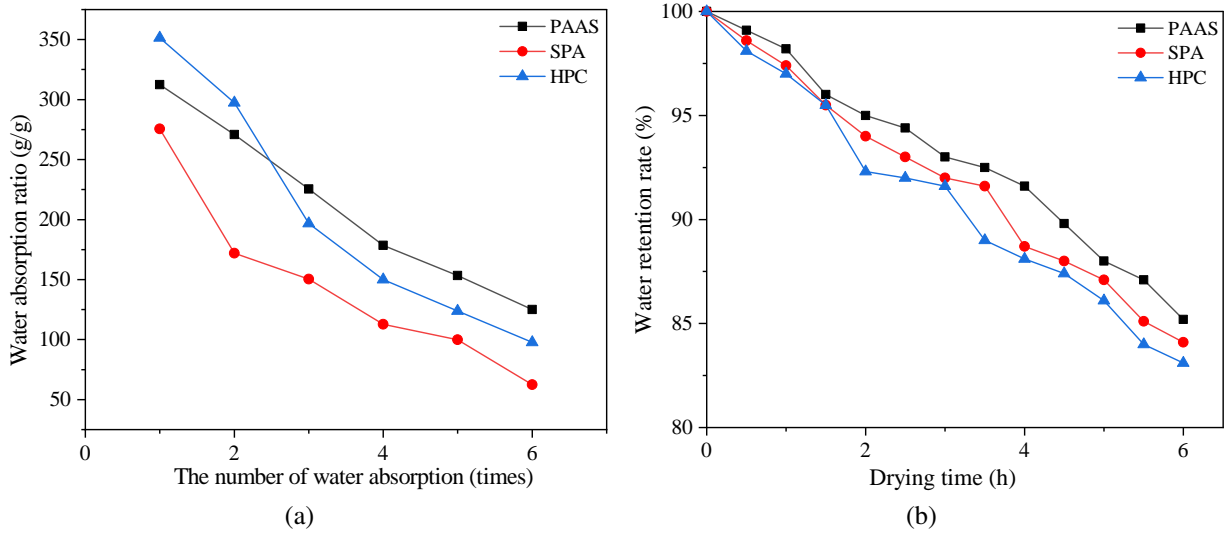
Fig. 8. Water absorption and moisturizing properties of water retaining agents: (a) water absorption effect and (b) water retaining effect.

$$Y_1 = 9.2x_1 + 5.3x_2 + 0.2x_3 + 0.6x_4 + 1.8x_1x_2 - 8.8x_1x_3 \\ - 8.1x_1x_4 - 1.2x_2x_3 - 2.6x_2x_4 + 1.3x_3x_4 \tag{7}$$

The multivariate linear equation fitting the evaporation resistance is ($R^2 = 0.97$):

$$Y_2 = 0.7x_1 + 0.8x_2 + 0.8x_3 + 0.9x_4 + 0.2x_1x_2 + 0.1x_1x_3 \\ + 0.2x_1x_4 + 0.2x_2x_3 + 0.1x_2x_4 + 0.1x_3x_4 \tag{8}$$

The multivariate linear equation fitting the surface tension is ($R^2 = 0.96$):

$$Y_3 = 30.6x_1 + 26.3x_2 + 84x_3 + 85.8x_4 + 2x_1x_2 - 39x_1x_3 \\ - 55.2x_1x_4 - 35x_2x_3 - 60x_2x_4 - 0.1x_3x_4 \tag{9}$$

The multivariate linear equation fitting the contact angle is ($R^2 = 0.9284$):

$$Y_4 = 21.5x_1 + 35x_2 + 83.5x_3 + 81x_4 - 27x_1x_2 - 50x_1x_3 \\ + 22x_1x_4 - 55x_2x_3 - 91.4x_2x_4 - 26.4x_3x_4 \tag{10}$$

The R^2 values of Eqs. (7)-(10) are close to 1, which indicates a good correlation between the independent variable and the dependent variable. The response surface changes of sedimentation rate, evaporation resistance, surface tension and contact angle are respectively 98.2%, 97.1%, 95.9%, and 92.8%. The results of variance analysis are shown in Table 4. The F values represent the main effect relationship on the response value. Generally, the larger the F value, the more significant the model. The P values represent the significance of the correlation coefficient. It can be seen that the model has a significant impact on the Y_1, Y_2, Y_3, Y_4 value when the P value is less than 0.05.

The P-value less than 0.05 indicates significance, while the P-value less than 0.01 indicates extreme significance. The linear fitting P-values of the models are all less than 0.05, which indicates that the models have high goodness of fit. The mismatch term represents the degree of fit between the model and the experiment. If the P-value of the mismatch term

is higher than 0.05, which indicates that the model established is consistent with the actual situation and can be used as an analysis and prediction model for the experiment. When the signal to noise ratio of the mixture design model is higher than 4, the model is considered reasonable, and the goodness of fit is high, which indicates the calculation results of response surface analysis are highly reliable.

The F values in Table 4 represent the degree of which the quality scores of independent variables x_1, x_2, x_3, and x_4 affect the dependent variables Y_1, Y_2, Y_3 and Y_4. Based on the experimental measurements data in Table 3 and response surface analysis data in Table 4, the conclusions can be drawn: in the mixed reagents, the influence of the interaction between the mixture A+C and the mixture A+D on the settling rate is as significant that of formula A and formula B on the settling rate of coal dust. Polymers have a synergistic effect on the wetting of coal dust with surfactants. Compared with a single surfactant, composite solutions can have a certain cementation effect and accelerate the sedimentation of coal dust. By analyzing the significance of the mix formulas A+B, A+C, A+D, B+C, B+D and C+D, it can be seen that the goodness of fit of A+C and A+D (P < 0.05) is higher than others (P > 0.05). It is indicated that the interaction between dust suppressant A, C and D has a significant impact on sedimentation rate.

The proportion of D in the mixed reagent has a significant impact on the anti-evaporation performance of the reagent. The interaction between A+D, A+B and B+C has a significant impact on the evaporation resistance of the reagent. The anionic surfactant SDBS has an association effect with the polymer and has a synergistic effect on the water retention performance of the reagent. By analyzing the significance of A+B, A+C, A+D, B+C, B+D and C+D items, it can be concluded that A+D, A+B, B+C items are significant (P < 0.05), while other items are not significant (P > 0.05). It means that the interaction between other dust suppressant components

Table 4. Model variance analysis.

Project source	Y_1		Y_2		Y_3		Y_4	
	F value	P value	F value	P value	F value	P value	F value	P value
Model	30.41	0.0008	18.59	0.0025	13.30	0.0054	7.21	0.0213
A+B	0.4269	0.5424	7.85	0.0379	0.0036	0.9544	0.3716	0.5688
A+C	10.08	0.0247	2.80	0.1549	1.38	0.2924	1.28	0.3090
A+D	8.65	0.0322	14.25	0.0130	2.83	0.1531	0.2452	0.6415
B+C	0.1982	0.6748	19.05	0.0073	1.14	0.3347	1.56	0.2668
B+D	0.8817	0.3909	3.41	0.1239	3.31	0.1287	4.33	0.0920
C+D	0.2205	0.6584	1.90	0.2263	0.0000	0.9968	0.3600	0.5747
Signal/noise	18.37		15.38		10.28		13.21	
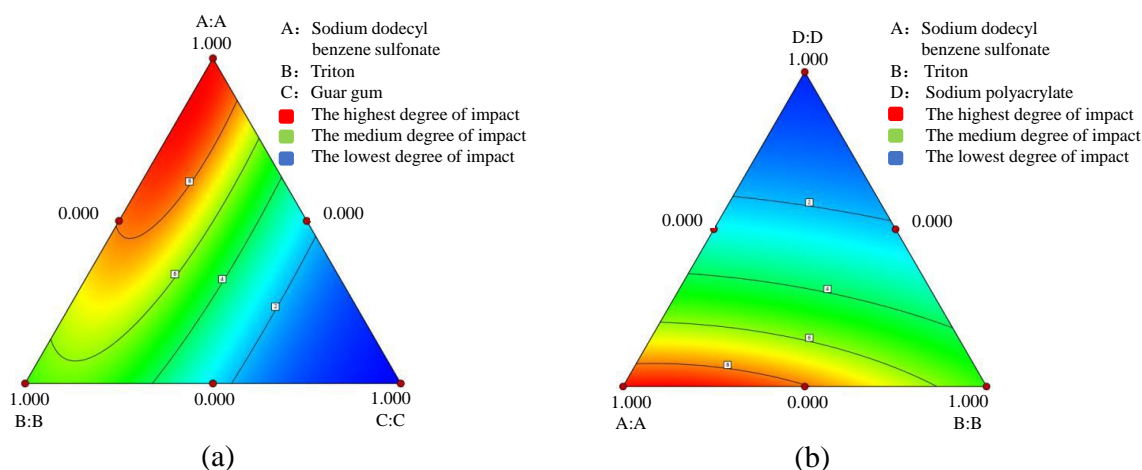
Fig. 9. 3D response contour of raw materials (a) A, B, C and (b) A, B, D.

has a small impact on evaporation resistance.

The surface tension of the reagent is impacted by several factors. Surfactants A and B promote the reduction of the reagent surface tension, while polymer polymers C and D hinder the reduction of the reagent surface tension. By analyzing the significance of A+B, A+C, A+D, B+C, B+D and C+D items, it can be concluded that each item is not significant (P > 0.05), and the impact of each component on the surface tension of dust suppressants is relatively small.

Surfactants A and B can promote the reduction of the contact angle between the solution and coal powder, and polymers C and D hinder the reduction of the surface tension between the solution and coal powder. Although various factors have an impact on the contact angle of the reagent, it was found that BD was a significant item (P < 0.05), while the other items were not significant (P > 0.05) by analyzing the significance of A+B, A+C, A+D, B+C, B+D and C+D. It is indicated that the interaction between other reagents had little effect on the antenna. The analysis results of response surface are shown from Fig. 9 to Fig. 12. In these figures, both points 1.000 and points (1.000) present the quality score of the formula in the model, and so on.

3.2.1 Interaction analysis of sedimentation rate

The three-dimensional (3D) response surface and contour map of the response values are obtained based on the multi-variate linear fitting equation, and further explore the impact of the interaction between independent variable components on the dependent variable.

According to Fig. 9, the contour map near A:A is the highest point of the graph, which is the highest point of the 3D response surface map. It is indicated that the coal dust deposition rate is the fastest here. The color change span from A:A to C:C shown in Fig. 9(a) and from A:A to D:D shown in Fig. 9(b) is large, which indicates that the reactions between sodium dodecyl benzene sulfonate and guar gum, as well as between sodium dodecyl benzene sulfonate and sodium polyacrylate, have a significant impact on the sedimentation rate of the composite solution.

3.2.2 Interaction analysis of Anti evaporation

According to Fig. 10(a), the middle of between B(1.000) and C(1.000) in the contour map near D is the highest point of the graph, which is the highest point in the 3D response surface map. This indicates that the reagent has the best evaporation
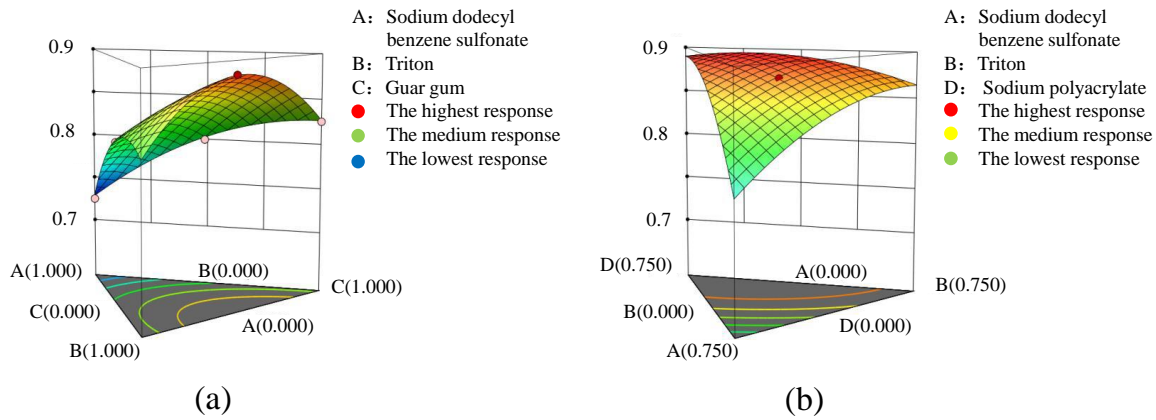
Fig. 10. 3D response curve of raw materials (a) A, B, C and (b) A, B, D.
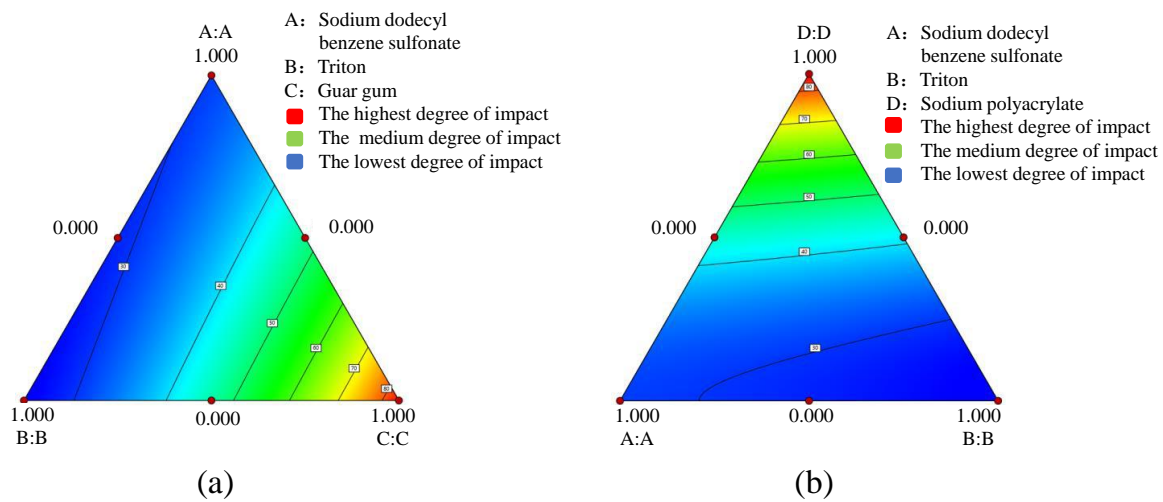
Fig. 11. 3D response contour of raw materials (a) A, B, C and (b) A, B, D.

resistance and water retention performance. Judging from the range of in Fig. 10(b), the color change span of from A(0.750) to D(0.750) is large. It is further indicated that the reactions between sodium dodecylbenzene sulfonate and sodium polyacrylate has a greater impact on the evaporation resistance of the mixed dust suppression agent solution.

3.2.3 Interaction analysis of surface tension

According to Fig. 11, there is the lowest point in the graph near B:B in the contour map, which is the lowest point in the 3D response surface map. It is indicated that the surface tension of the coal sample here is the smallest. The range of color changes from from B:B to C:C shown in Fig. 11(a), as well as from from B:B to D:D shown in Fig. 11(b) is large. It is concluded that the reactions between triton and guar gum, as well as between triton and sodium polyacrylate have a significant impact on the surface tension range of the mixed dust suppressor solution.

3.2.4 Interaction analysis of contact angle

According to Fig. 12, the point near A(1.000) in the contour map is the lowest point in the graph, which is the

lowest point in the 3D response surface map. It indicated that the solution here has the smallest contact angle with pulverized coal. The range of color changes from A(1.000) to C(1.000) in Fig. 12(a), as well as from A(1.000) to D(1.000)in Fig. 12(b) are is large. It is indicated that the reactions between sodium dodecyl benzene sulfonate and guar gum, as well as between sodium dodecyl benzene sulfonate and sodium polyacrylate have a significant impact on the contact angle of the mixed dust suppression agent solution.

3.2.5 Optimization formula results and optimization

According to the optimization analysis based on the mixture design model, the reagent sedimentation rate and evaporation resistance performance are directly proportional to the dust reduction effect, and the surface tension and contact angle are inversely proportional to the dust reduction effect. Therefore, by analyzing the optimization, the maximum upper limit value of sedimentation rate and evaporation resistance performance are selected, while the minimum lower limit value of surface tension and contact angle are selected. The optimal ratio of the dust suppressant mixture design model is obtained as: 39.8% for sodium dodecyl benzene sulfonate,
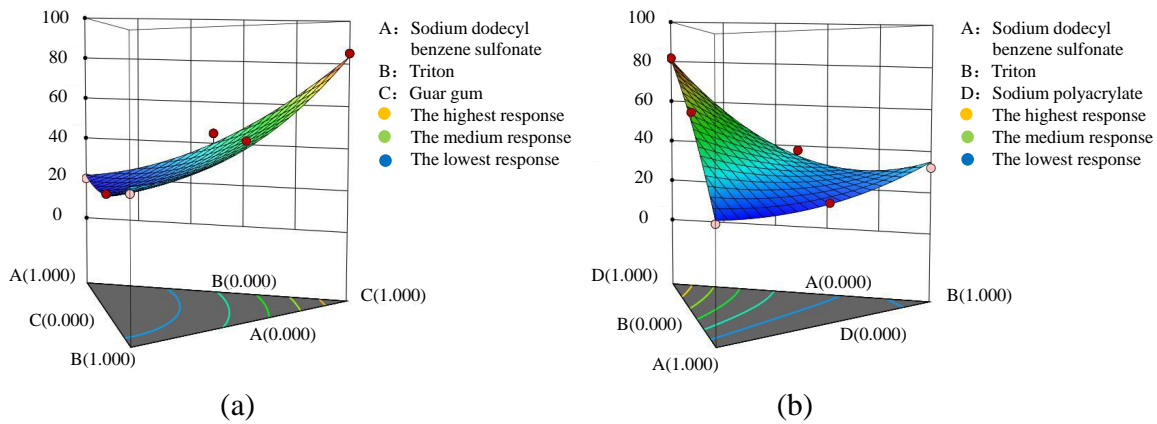
Fig. 12. 3D response curve of raw materials (a) A, B, C and (b) A, B, D.

Table 5. Comparison results of optimized value and measured value.

Factors	Y_1 (mg/s)	Y_2 (%)	Y_3 (mN/m)	Y_4 (°)
Theoretical value	6.56	83	30	24
Measured value	6.42	85	29	26
Error	2.1%	2.4%	3.3%	8.3%
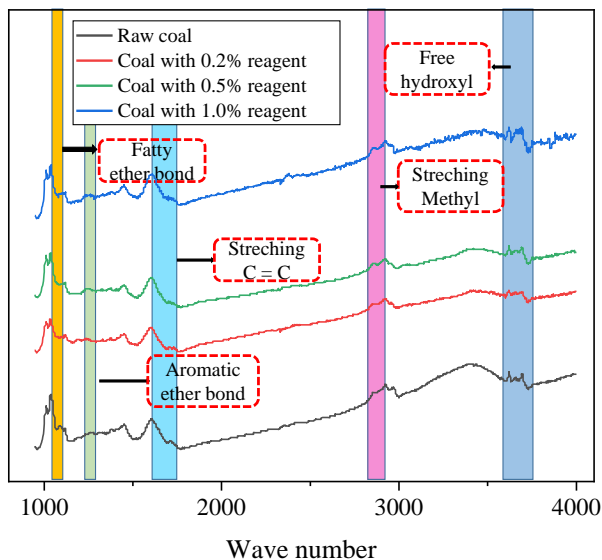
Fig. 13. Infrared spectrum characterization results of coal dust.

rate, evaporation resistance, surface tension, and contact angle are basically consistent with the theoretical results of the model. The error of the first three items values are within 5%. However, the error of the contact angle is 8.3%, which is relatively larger than other error values. The reason for this result is that the spreading of liquid droplets on the mine sample is easily affected by the variations in surface energy and the surface roughness of the coal body. It results in a difference of 2 degrees between the measured value and theoretical value of the contact angle. Based on research experience, it is reasonable for the error between the measured value and the theoretical value to be less than 10%. Therefore, the ratio of the dust suppressant mixture (39.8% for sodium dodecyl benzene sulfonate, 53% for triton, sodium dodecyl benzene sulfonate, 3.9% for guar gum, 3.3% for sodium polyacrylate) can be selected as the optimal formulation of dust suppressant.

3.3 Characterization of the optimal formula

3.3.1 Chemical bond changes

The infrared spectra of raw coal and coal samples after dust suppression treatment are shown in Fig. 13.

Due to the occurrence of multiple peaks overlapping in the absorption peaks of various functional groups in coal, it is necessary to perform peak splitting and disaggregation fitting for the infrared spectrum. After correcting the baseline of the infrared spectrum, peak fit software is used to fit the main absorption peaks of raw coal and processed coal samples. According to the absorption peak areas corresponding to the characteristic functional groups, the changes of the functional group content of raw coal are compared before and after dust

53% for triton, 3.9% for guar gum, and 3.3% for sodium polyacrylate. At this ratio, the reagent concentration is diluted to 0.1%. The theoretical values of the formula's sedimentation rate, evaporation resistance, surface tension, and contact angle are 6.56 mg/s, 83%, 30 mN/m, and 24°, respectively.

In order to further verify the effectiveness and accuracy of this dust suppression agent mixing design model, four reagents were prepared at this ratio and diluted to 0.1%. The sedimentation rate, evaporation resistance, surface tension, and contact angle of the solution were measured, and compared with the optimized results. The results are shown in Table 5.

It can be seen that the measured values of sedimentation

suppression treatment to obtain Fig. 13.

The effect of dust suppressants on pulverized coal mainly considers three typical functional groups, namely hydroxyl, ether bond, and aromatic hydrocarbon, on the surface of coal molecules before and after the action. Quantitative analysis is conducted by using the 3,700 to 3,100 cm^{-1} bond with hydroxyl as the main functional group in the infrared spectrum, and the 1,800 to 1,000 cm^{-1} band with aromatic hydrocarbons and most of the main oxygen-containing functional groups.

The pulverized coal samples before and after treatment showed three distinct absorption peaks at a wavelength greater than 3,600 cm^{-1}, which is belonged to the stretching vibration of free hydroxyl groups. At 3,400 cm^{-1}, two stretching vibration absorption peaks belonging to associative hydroxyl groups appeared, including stretching vibration of phenols, alcohols, carboxylic acids, peroxides and hydroxyl groups in water. There is a significant absorption peak of carbon-carbon double bond stretching vibration in aromatic hydrocarbons at 1,600 cm^{-1}, and the peak area reflects the aromatic ring content in coal. There is a small region of olefin vibration at 1,600~1,700 cm^{-1}, and a wide overlapping peak of carbon oxygen bond ether bonds appears at 1,400~1,000 cm^{-1}. The absorption peaks within 1,150~1,060 cm^{-1} wave numbers belong to fatty ether bonds, and the absorption peaks within 1,270~1,230 cm^{-1} wave numbers belong to aromatic ether bonds.

After coal sample treatment, the peak area at 3,650~3,600 cm^{-1} was significantly reduced, and the peak area of the hydroxyl stretching vibration peak at 3,400 cm^{-1} was significantly reduced. Hydroxyl is a class of active functional groups that have a significant impact on coal sedimentation efficiency. The nonionic wetting agent triton has a significant effect on the content of the hydrophilic functional group hydroxyl in coal dust. After absorbing water, the water retaining agent sodium polyacrylate fixes the water molecules on the polymer chain, ensuring that no water is lost. When reacting with water, more hydrogen bonds can be formed. Hydroxyl groups are polar hydrophilic groups, and the main body of coal molecules is a low polar carbon skeleton. The presence of hydroxyl groups in the side chains makes it easier for water molecules to adsorb and improve their hydrophilicity. However, due to the relatively small bond energy of the hydroxyl bond itself, the hydrogen ions in the hydroxyl group are not stable enough and prone to ionization. The number of this functional group varies greatly before and after coal sample treatment. After treatment, the peak areas of the antisymmetric stretching vibration peak of methyl at 2,889 cm^{-1} and the symmetric stretching vibration peak of methyl at 2,836 cm^{-1} decreased. Aliphatic hydrocarbons are hydrophobic, and the decrease in the peak area of aliphatic hydrocarbons indicates that the dust suppressor formula reduces the hydrophobicity of the coal sample. After treating the coal sample, the peak areas of several carbon-carbon double bond stretching vibrations in olefins and aromatic hydrocarbons (ranging from 1,760 to 1,680 cm^{-1}) have exhibited varying degrees of reduction. Additionally, multiple carbon-carbon double bond stretching vibration peaks in aromatic hydrocarbons between 1,570 and 1,700 cm^{-1} are observed. The aromatic skeleton is the main

structure of coal, and it has the weak functional group polarity. The reaction between the dust suppressor solution and the coal sample has changed some of the coal skeleton. Following the treatment of the coal sample, the peak areas associated with aromatic ether bonds (1,230 to 1,270 cm^{-1}) and fatty ether bonds (1,060 to 1,150 cm^{-1}) exhibited an increase in comparison to untreated pulverized coal. This suggests an elevation in oxygen-containing functional groups within the coal sample, leading to heightened hydrophilicity and improved dust suppression performance. The ether bond is a stable group formed by the etherification reaction between the dust suppression agent solution and the groups in the coal sample. It indicates that the coal sample treated with dust suppressant can block the chain reaction of free radicals, thereby improving the stability of the coal sample.

The infrared experimental results have shown that adding dust suppressants to coal dust significantly increases its hydrophilicity, and the higher the concentration of dust suppressants added, the stronger the hydrophilicity. However, the concentration of the reagent used in the dust suppressant spraying experiment also depends on the viscosity of the dust suppressant solution. Excessive concentration of composite dust suppressants will increase their viscosity, making it impossible to spray. Considering the feasibility of spraying dust suppressants on the equipment, a 0.1% concentration dust suppressant solution was selected for the final simulation spraying experiment, ensuring the sustainable spraying of the reagent while meeting the dust reduction requirements.

3.3.2 Electron microscopic characterization results of coal samples

The coal samples were characterized by scanning electron microscope. It can be observed that the surface morphology of the coal samples after spraying water and dust inhibitor is different. The comparison of the scanning electron microscope is shown in Fig. 14.

Figs. 14(a)-14(b) are the structural shapes of coal dust that are magnified by 200 and 300 times respectively after spraying water. There are many voids and folds on the surface of the coal body, and the particles are very dispersed. Figs. 14(c)-14(d) are the structural shapes of coal dust that are magnified by 200 and 300 times respectively after spraying dust suppressant. There are almost no voids between the particles of the coal body. The diameter of individual particles increases significantly. The particles of the coal body bind together that makes the surface of coal become smooth. The Fig. 14(a) depicts that, after water spraying, most of the coal dust particles in the samples exhibit smaller sizes, loosely distributed within the visible range. The gaps between adjacent particles are substantial, and the surface appears relatively rough. In Fig. 14(c), compared to 14(a), the gaps between adjacent coal dust particles in the samples treated with a optimize formula dust suppressant are significantly reduced. Many fine particles adhere to the surface of the coal dust, and some small particles of coal dust can be clearly observed aggregating together to form larger particles. Fig. 14(d) illustrates the morphology of the modified dust particles. In comparison to Fig. 14(b), it is evident that the particles formed by aggregation
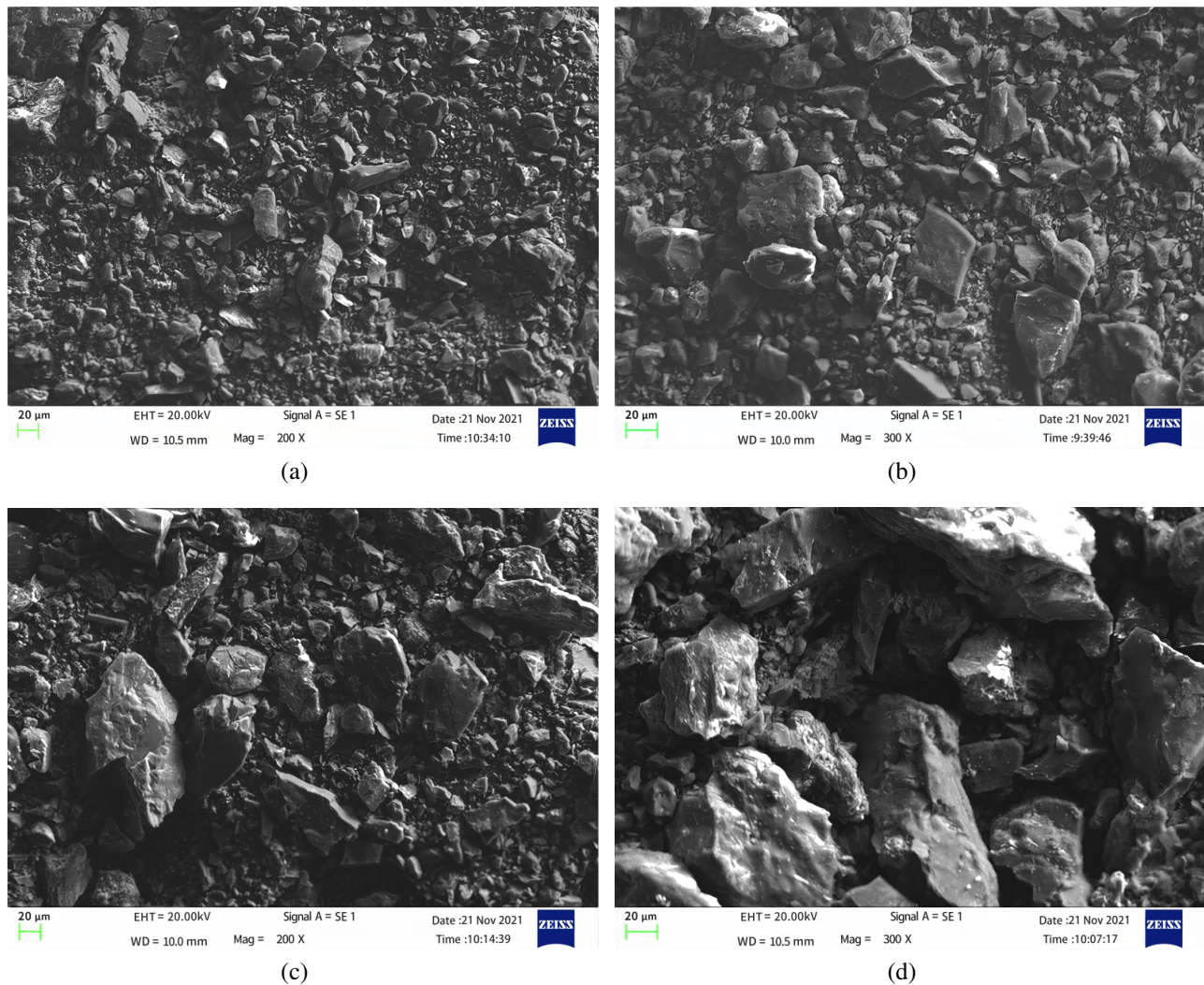
Fig. 14. Comparison of SEM results of dust suppressants: (a) × 200 spray water, (b) × 300 spray water, (c) × 200 spray dust suppressant and (d) × 300 spray dust suppressant.

Table 6. Acute inhalation toxicity test results in SD rats.

Gender	Body mass after inhalation					Maximum tolerable dose
	Initial	1 day	3 days	7 days	14 days	
Male	303.6±2.9	304.2±6.3	311.1±3.3	329.9±5.1	364.7±3.8	>10 mg/L
Female	281.9±4.3	283.0±5.1	289.9±6.9	297.7±3.6	315.4±4.2	>10 mg/L

are larger and denser. The surface of the coal dust clearly shows a thin film generated due to the outstanding adhesive properties of the composite dust suppressant. The composite dust suppressant can adhere to the surface of coal dust particles or occupy the pores of coal dust particles, thereby reducing the porosity of the coal dust. Based on the characterization results of coal powder, it can be seen that dust suppressants can improve the wettability and adhesiveness of coal dust. Besides that, adhesion between coal particles and the formation of a solidified film on the surface can further inhibit the occurrence of secondary dust.

3.3.3 Toxicity analysis of dust suppressant

The changes in body mass of the tested rats are shown in Table 6.

Female and male SD rats showed no obvious poisoning symptoms or death within 2 weeks after inhalation exposure, and their body mass did not show any significant changes. This experiment indicates that the maximum tolerable of the dust suppressant component in the acute inhalation test of female and male SD rats is greater than 10.0 mg/L. According to the identification standard of GB5085.2-2007 and the acute toxi-
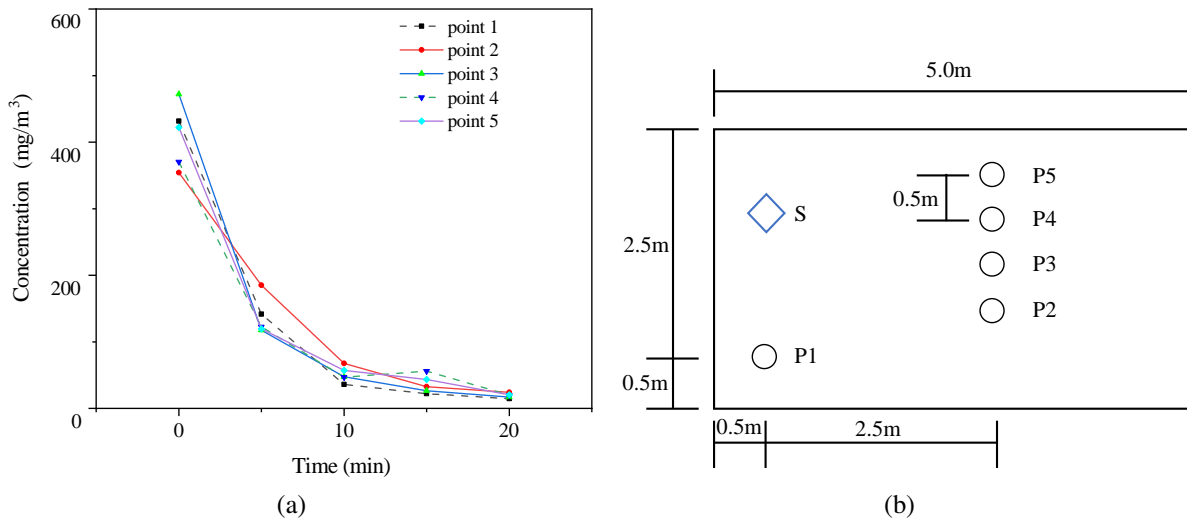
Fig. 15. Dust concentration change of dust measure points.(a) Concentration changes and (b) Location map of measuring points.
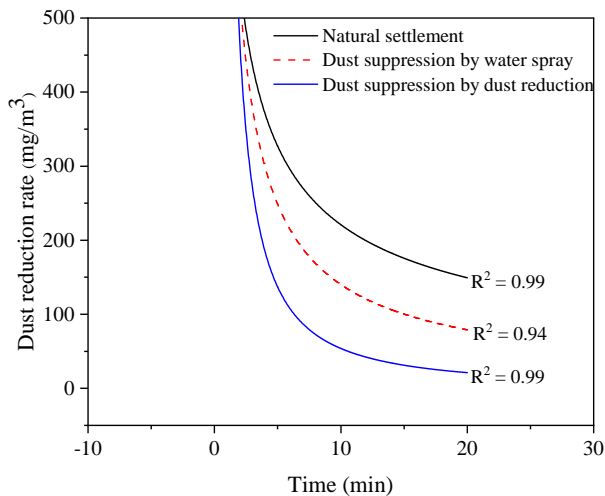
Fig. 16. Dust concentration change of dust suppressor.

city half lethal classification standard, if the half lethal concentration of steam, smoke, or dust inhalation toxicity is more than 10 mg/L, it is determined to be non-toxic.

3.4 Analysis of dust reduction efficiency

The layout of the measurement points is shown in Fig. 15(b). The dust suppressant spraying device is installed at point S. The installation positions of measurement points 1-5 are shown in it. Measurement point 2 is the farthest from the implementation of dust reduction in a straight line. In the initial state, the dust concentration at each measuring point in the space ranges from 354 to 472 mg/m^3. After spraying dust suppressant, the dust concentration in the space decreases over time, rapidly decreasing within the first 5 minutes. The dust concentration at measurement point 2 decreases the slowest. The slope of the decrease curve in the first 5 minutes of dust reduction is 47.7, and the slope of the concentration decrease at other measurement points from 0 to 5 minutes exceeds 67. The dust concentration decreases gradually and becomes stable

within 5 to 10 minutes, and it decreases from 14.5 to 24 mg/m^3 within 20 minutes.

It can be seen from Fig. 16 that the average dust concentration in the space under the initial state is 454.6, 431 and 410 mg/m^3, respectively. The coal dust in the space is treated by natural sedimentation, water spray and dust suppression agent spray. By the three methods, the dust concentration decreases over time, and at the time of the test termination, the dust concentration in the space is 149.0, 64.2, and 19.2 mg/m^3, respectively.

Within 5 minutes after dust reduction, the concentration of coal dust in the space decreases at an extremely fast rate, with the decline rates at 58, 38.6, and 26.6 respectively. The reason is the high concentration of coal dust in the space and the large number of particles that are easily captured by fog droplets during the early stage of dust reduction. In the later stage of dust reduction, the concentration of coal dust in the space becomes lower and lower, and the number of particles becomes smaller, which makes it difficult to capture dust coal. The sedimentation efficiency of the three dust suppression methods within 20 minutes was calculated to be 67.2%, 85.1%, and 95.3%, respectively. The dust suppression efficiency of spray is 28.1% and 10.2% which are higher than that of natural sedimentation and water spray, respectively. In the whole process of dust suppression for 20 minutes, the dust suppression agent spray dust reduction rate is always greater than that of the other two dust suppression methods. The dust suppression agent spray can make the solution be easier to combine with the dust, and make the dust settle quickly in a short time.

4. Conclusions

1) Using the mixture design model designed by the Design-expert 13 software, 15 schemes were proposed for mixture design. Experiments were carried out on the sedimentation rate, evaporation resistance, surface tension,

and coal dust contact angle performance of dust suppressants at different ratios. Based on the response surface analysis results, it is observed that the settling rate (Y_1) and anti-evaporation property (Y_2) exhibit a synergistic relationship, which contributes to the dust suppression effectiveness of the dust suppressant. Conversely, surface tension (Y_3) and contact angle (Y_4) demonstrate an antagonistic relationship, which influences the dust suppression effectiveness of the dust suppressant. The optimal ratio was determined as 39.8% for sodium dodecyl benzene sulfonate, 53% for triton, 3.9% for guar gum, and 3.3% for sodium polyacrylate.

2) The dilution ratio of the dust suppressant to water used in the experiment is 99.9 : 0.1. The IR characterization results show that the concentration of the dust suppressant has a significant effect on the content of hydrophilic functional groups, hydroxyl groups, and hydrophobic ether bonds in coal dust. The SEM characterization results show that the dust suppressant has good wettability and adhesion to coal seams, and a strong encapsulation ability to coal dust.

3) The initial dust concentration of the three groups of natural sedimentation, water spray dust suppression and dust suppression agent spray dust suppression tests are divided into 454.6, 431 and 410 mg/m^3. The dust concentrations after 20 minutes of dust suppression are 149.0, 64.2 and 19.2 mg/m^3, respectively. The sedimentation efficiency of the three dust reduction methods was 67.2%, 85.1%, and 95.3%, respectively. The dust suppression efficiency of dust suppression agent spray is 28.1% and 10.2% which is higher than that of natural sedimentation and water spray, respectively.

The optimized formula dust suppressant obtained in this study significantly improves the efficiency of mine dust reduction. In the future, the research on the optimization formula of composite and environmental dust suppressants will be carried out, aiming to further improve the dust reduction efficiency of dust suppressants and reduce the cost of dust suppressants and the pollution to the environment.

Acknowledgements

Conflict of interest

The authors declare no competing interest.

References

Abdel Rahem, R. A. Dilute hydrochloric acid induced switching from antagonism to synergism in the binary mixed systems of cocamidopropyl betaine (CAPB) and sodium dodecyl benzene sulfonate (SDBS). Tenside Surfactants Detergents, 2023, 60(3): 223-230.

Alrweilih, H., Georgiou, S. D., Stylianou, S. A new class of second-order response surface designs. IEEE Access, 2020, 8: 123-132.

Amato, F., Querol, X., Johansson, C., et al. A review on the effectiveness of street sweeping, washing and dust suppressants as urban PM control methods. Science of The Total Environment, 2010, 408(16): 3070-3084.

Azam, S., Mishra, D. P. Effects of particle size, dust concentration and dust-dispersion-air pressure on rock dust inertant requirement for coal dust explosion suppression in underground coal mines. Process Safety and Environmental Protection, 2019, 26: 35-43.

Chaker, H., Attar, A. E., Djennas, M., et al. A statistical modeling-optimization approach for efficiency photocatalytic degradation of textile azo dye using Cerium-do oed mesoporous ZnO: A central composite design in response surface methodology. Chemical Engineering Research and Design, 2021, 171: 198-212.

Deng, L., Ge, X., Fan, G., et al. Quantitative analysis of minerals based on scanning electron microscopy energy dispersive spectroscopy: Using AMICS as an example. World Nuclear Geological Science, 2023, 40 (1): 98-105. (in Chinese)

Dudek, M., Olsen, A. O. J., Øye, G. The influence of divalent cations on the dynamic surface tension of sodium dodecylbenzenesulfonate solutions. Colloids and Surfaces A: Physicochemical and Engineering Aspects, 2023, 675: 132007.

Eades, R., Perry, K., Johnson, C., et al. Evaluation of the 20 L dust explosibility testing chamber and comparison to a modified 38 L vessel for underground coal. International Journal of Mining Science and Technology, 2018, 28(6): 885-890.

Eckhoff, R. K., Li, G. Industrial dust explosions, a brief review. Applied Sciences, 2021, 11(4): 1669.

Geetha, D., Thilagavathi, T., Ramesh, S. P., et al. Influence of synthetic polymer on aqueous anionic surfactant (SDBS) micelle investigated by FT-IR and ultrasonic study. Composite Interfaces, 2010, 17(2-3): 247-256.

He, S., He, X., Mitri, H., et al. Advances in mining safety theory, technology, and equipment. Advances in Geo-Energy Research, 2023, 10(2): 71-76.

Huang, Z., Huang, Y., Yang, Z., et al. Study on the physicochemical characteristics and dust suppression performance of new type chemical dust suppressant for copper mine pavement. Environmental Science and Pollution Research, 2021, 28(42): 59640-59651.

Kan, J., Xie J., Guo, Y. Analysis of dust concentration and particle size measurement in coal mine underground. Journal of Taiyuan University of Technology, 2017, 48 (4): 592-597. (in Chinese)

Kumykov, V. K., Kumykova, T. M. Fire-hazardous ore mining and stockpiling technology. Journal of Mining Science, 2013, 49(4): 598-603.

Kunz, B. K., Little, E. E., Barandino, V. L. Aquatic toxicity of

chemical road dust suppressants to freshwater organisms. Archives of Environmental Contamination and Toxicology, 2021, 82(2): 294-305.

Li, M., Tang, J., Song, X., et al. Optimization model out of suppressant component ratio based on response surface methodology. China Safety Science Journal, 2023, 33(1): 88-94. (in Chinese)

Li, P., Yu, D., Tam, S. The experience of patients and family caregivers in managing pneumoconiosis in the family context: A study protocol. Journal of Advanced Nursing, 2019, 75(12): 3805-3811.

Liang, W., Zhang, Z., Yang, Y., et al. Preparation and performance investigation of road dust suppressant with straw enzymatic hydrolysate. Fresenius Environmental Bulletin, 2022, 31(8B): 9231-9243.

Luo, R., Lin, M., Luo, Y., et al. Preparation and properties of a new type of coal dust suppressant. Journal of China Coal Society, 2016, 41(s2): 454-459. (in Chinese)

Pan, L., Golden, S., Assemi, S., et al. Characterization of particle size and composition of respirable coal mine dust. Minerals, 2021, 11(3): 276.

Perera, I. E., Harris, M. L., Sapko, M. J., et al. Large-Scale explosion propagation testing of treated and non-treated rock dust when overlain by a thin layer of coal dust. Mining, Metallurgy & Exploration, 2021, 38(2): 1009-1017.

Qiu, L., Zhu, Y., Liu, Q., et al. Response law and indicator selection of seismic wave velocity for coal seam outburst risk. Advances in Geo-Energy Research, 2023, 9(3): 198-210.

Rakhi, T., Vineet, K., Pradeep, S., et al. Hydroxypropylation of 1, 2 Galactomannan by Taguchi's L9 orthogonal array design. Chemistry Select, 2021, 6(33): 8709-8715.

Ray, K. S., Khan, M. A., Mohalik, K. N., et al. Review of preventive and constructive measures for coal mine explosions: An Indian perspective. International Journal of Mining Science and Technology, 2022, 32(3): 471-485.

Rolf, K. E., Li, G. Industrial dust explosions, A brief review. Applied Sciences, 2021, 11(4): 1669.

Sah, R., Dutta, S. K. Effects of binder on the properties of iron ore-coal composite pellets. Mineral Processing and Extractive Metallurgy Review, 2010, 31(2): 73-85.

Sartore, L., Pandini, S., Baldi, F., et al. Biocomposites based on poly (lactic acid) and superabsorbent Sodium polyacrylate. Journal of Applied Polymer Science, 2017, 134(48): 45655.

Shao, H., Hu, H., Lu, Q. Experimental study on water retention and flame retardancy of environmental protection slurry of film coated gasification slag. Combustion Science and Technology, 2023, in press, https://doi.org/10.1080/00102202.2023.2168539.

Shi, G., Han, C., Wang, Y., et al. Experimental study on synergistic wetting of a coal dust with dust suppressant compounded with noncationic surfactants and its mechanism analysis. Powder Technology, 2019, 356: 1077-1086.

Smita, S., Pandey, J. P., Sen, G. Microwave assisted synthesis of guar gum based biopolymeric macromolecule optimized as a flocculant for mineral ore processing. International Journal of Biological Macromolecules, 2022, 220: 307-315.

Tessum, M. W., Raynor, P. C. Effects of spray surfactant and particle charge on respirable coal dust capture. Safety and Health at Work, 2017, 8(3): 296-305.

Tsai, Y. T., Yang, Y., Huang, H., et al. Inhibitory effects of three chemical dust suppressants on nitrocellulose dust cloud explosion. AIChE Journal, 2020, 66(5): e16888.

Tsogt, B., OH, S. Y. Preparations and application of dust suppressants from biomass-based materials. Journal of the Air & Waste Management Association, 2021, 71(11): 1386-1396.

Wang, C., Liu, Y., Song, D., et al. Evaluation of bedding effect on the bursting liability of coal and coal-rock combination under different bedding dip angles. Advances in Geo-Energy Research, 2024, 11(1): 29-40.

Wang, H., Jia, J., Jiang, Z., et al. Analysis of health service utilization and its influencing factors among patients with pneumoconiosis in China. Biomedical and Environmental Sciences, 2021, 34(1): 83-88.

Wu, Q., Tang, T., Zhao, Z., et al. Influence of micro-particles on gas hydrate formation kinetics: Potential application to methane storage and transportation. Advances in Geo-Energy Research, 2023, 10(3): 189-199.

Xi, Z., Feng, Z., Li, A. Synergistic coal dust control using aqueous solutions of thermoplastic powder and anionic surfactant. Colloids and Surfaces A Physicochemical and Engineering Aspects, 2017, 520: 864-871.

Yang, Y., Zhao, Q., Mi, Y. Preparation and optimum proposal of biological dust suppressant using straw based on orthogonal test. Journal of Highway and Transportation Research and Development (English Edition), 2021, 15(2): 8-17.

Zhang, H., Nie, W., Yan, J., et al. Preparation and performance study of a novel polymeric spraying dust suppression agent with enhanced wetting and coagulation properties for coal mine. Powder Technology, 2020, 364: 901-914.

Zhang, Y., Li, J., Tian, Y., et al. Virtual water flow associated with interprovincial coal transfer in China: Impacts and suggestions for mitigation. Journal of Cleaner Production, 2021, 289: 125800.

Zhao, Y., Wang, K., Xu, L., et al. The effect of mining dust suppressants on the wetting performance of coal dust with different particle sizes. Shanxi Coal, 2023, 42(5): 49-53. (in Chinese)

Zhou, L., Yang, S., Yuan, Z., et al. Inhibition of fine particles fugitive emission from the open-pit lignite mines by polymer aqueous solutions. Colloids & Surfaces A Physicochemical & Engineering Aspects, 2018, 555: 429-439.